

Interpretation of photoemission spectra of $(\text{TaSe}_4)_2\text{I}$ as evidence of charge-density-wave fluctuations

This article has been downloaded from IOPscience. Please scroll down to see the full text article.

1996 J. Phys.: Condens. Matter 8 10493

(<http://iopscience.iop.org/0953-8984/8/49/037>)

View [the table of contents for this issue](#), or go to the [journal homepage](#) for more

Download details:

IP Address: 171.66.16.207

The article was downloaded on 14/05/2010 at 05:50

Please note that [terms and conditions apply](#).

Interpretation of photoemission spectra of $(\text{TaSe}_4)_2\text{I}$ as evidence of charge-density-wave fluctuations

Nic Shannon[†] and Robert Joynt[‡]

[†] Department of Physics, University of Warwick, Coventry, UK

[‡] Department of Physics, University of Wisconsin–Madison, 1150 University Avenue, Madison, WI 53706, and Department of Technical Physics, Helsinki University of Technology, 02150-Espoo, Finland

Received 8 June 1996, in final form 4 September 1996

Abstract. The competition between different and unusual effects in quasi-one-dimensional conductors makes the direct interpretation of experimental measurements for these materials both difficult and interesting. We consider evidence for the existence of large charge-density-wave fluctuations in the conducting phase of the Peierls insulator $(\text{TaSe}_4)_2\text{I}$, by comparing the predictions of a simple Lee, Rice and Anderson theory for such a system with recent angle-resolved photoemission spectra. The agreement obtained suggests that many of the unusual features of these spectra may be explained in this way. This view of the system is contrasted with the behaviour expected of a Luttinger liquid.

1. Introduction

Restriction of a many-body system to low dimension brings with it simplifications but also a cost—the need to pay much closer attention to the effects of both thermodynamic fluctuations and interparticle correlations. One-dimensional models have proved an extremely rich field for the exploration of subtle effects of electron–electron interactions. They have been found to have quite complex ground states brought about by the same reduced phase space which makes some of their properties soluble, and which causes finite temperature to play so dramatic a role.

A colourful variety of quasi-one-dimensional and two-dimensional materials are now accessible to experiment, but this has not produced scientific consensus in all areas. Nine years of intensive research on high-temperature superconductors, the best known examples of quasi-two-dimensional systems, have failed to yield agreement on even the symmetry of their respective ground states.

The study of quasi-one-dimensional conductors has been less intense, but they are interesting for similar reasons. All attempts to model these materials must make reference to the fact that they are not truly one-dimensional, but merely very, very anisotropic. The set of materials to which $(\text{TaSe}_4)_2\text{I}$ belongs have a common structure of an assembly of weakly coupled conducting chains. Their behaviour has generally been understood in terms of those properties of one- (or three-) dimensional systems which are held to be relevant to them. This interplay of dimensionality is not trivial; weak interchain coupling will act to stabilize states born of instabilities in the underlying one-dimensional structure, which would otherwise be destroyed at finite temperature by large thermodynamic fluctuations. In the limit of strong coupling both the instability and the fluctuations may be irrelevant.

Many and diverse experimental techniques have been brought to bear on quasi-one-dimensional conductors in pursuit of insight into their properties and the low-dimensional physics which these betray. The transition metal tetrachalcogenide $(\text{TaSe}_4)_2\text{I}$ alone, in the thirteen years since its first synthesis [1], has been probed with neutron scattering [2], x-rays [3], low-energy electrons [4], ultraviolet photons [5], and subjected to measurements of optical and electrical conductivity [6–8] and magnetic susceptibility [9]. This material is interesting, since on cooling it displays a second-order phase transition at the (relatively high) temperature of 263 K, from a highly conductive but extremely anisotropic ‘metallic’ phase into a semiconducting charge-density-wave ground state. While angle-integrated photoemission [10, 11] and inverse photoemission [12] experiments have been performed on such materials for some time, only very recently have angle-resolved photoemission (ARPES) data become available. These offer the most direct means yet of understanding the changes which take place in the system’s electronic properties.

The instability of one-dimensional metals against an insulating ground state was described by Peierls [13] in 1953 and the mean-field theory [14] can be constructed in close analogy to the BCS theory of superconductivity. It is also well known that the fluctuations forced by the restricted phase space of a truly one-dimensional system prevent it from undergoing a phase transition at any finite temperature. The real systems, then, must exhibit an interplay of dimensional and thermodynamic effects, which manifest themselves in the strong and unusual temperature dependence of the ‘metallic’ properties observed above the transition temperature. Early measurements of the magnetic susceptibility of $(\text{TaSe}_4)_2\text{I}$ [9] suggested that fluctuations of the charge-density-wave (CDW) order parameter were present for all temperatures above 263 K, up to the limit of the compound’s chemical stability (at about 430 K). In order to understand the phase transition which takes place in this and other similar materials, it is necessary first to understand the role of fluctuations in the properties of a one-dimensional conductor.

It has also been known for some time that the Landau Fermi-liquid state is unstable against interparticle interaction in one dimension; the paradigm of the Luttinger liquid has evolved to describe the properties of a number of abstract one-dimensional models (for an overview see [15]). Luttinger liquids have unusual correlation functions displaying separation of spin and charge degrees of freedom, and possess no stable single-particle excitations at the Fermi energy ϵ_F . This implies that the customary discontinuity in zero-temperature occupation number $n(k)$ at the Fermi wavevector k_F found in all Fermi liquids is absent, and that the electronic density of states will vanish near ϵ_F , with a power-law behaviour determined by the strength of interparticle interactions. The decoupling of spin and charge degrees of freedom manifests itself in new structure in the spectral function of the system.

A topic much discussed in recent years is whether some aspects of this well-established one-dimensional behaviour can survive in higher dimensionalities. For example, it has been proposed that the normal-state properties of high-temperature superconductors can be understood on the basis of this hypothesis [16], while others believe that any coupling between chains must destroy the Luttinger liquid. One approach to this problem is empirical: if evidence of Luttinger-liquid behaviour could be found for a real weakly-coupled-chain system this would constitute proof of the possibility of such behaviour in higher dimensions. In this spirit, we ask whether $(\text{TaSe}_2)_4\text{I}$ is, experimentally, a Luttinger liquid, as has sometimes been claimed. As a first step, we compare ARPES data with a more conventional interpretation, that of CDW fluctuations. In a later paper, we shall attempt a more systematic comparison of strongly correlated electron and CDW theories for the transport properties and the ARPES and core-level lineshapes of $(\text{TaSe}_2)_4\text{I}$.

In sections 2 to 4 of this paper we shall present the model used, its overall properties, and the comparison of theory and experiment for ARPES lineshapes in $(\text{TaSe}_4)_2\text{I}$. The discussion is based on the premise that fluctuation effects born of the electron–phonon interaction dominate over those of correlation (interparticle interaction) for this system. It is found that such a treatment works well for $(\text{TaSe}_2)_4\text{I}$. A critical comparison of this picture with other candidate descriptions is given in the conclusions of section 5.

2. The model

The problem of describing the combined effect of correlation and electron–phonon interaction in one dimension on an equal footing is an axiomatically hard one, since correlation in one dimension destroys the Fermi-liquid picture on which the (perturbative) treatment of electron–phonon interaction is based, whilst the physics of the Peierls transition is dictated by $2k_f$ ‘backscattering’ events, which cannot be treated within the usual scheme for electronic correlations. For a given real material, in a given temperature range, however, it may not be necessary to solve the general problem in order to understand the results of experiment. As there is no clear framework for relating the microscopic properties of materials to the parameters of *any* of the phenomenological models referred to in this paper, the best that can be done is to develop a model based on what is believed to be the relevant subset of physics for each material, and to test it against a variety of experiments.

In order to provide a framework for our calculation we briefly review here some basic perturbative (mean-field) results for electrons in a Peierls CDW system, and present a succinct derivation of a Green’s function for electrons suffering fluctuations of CDW order, in the spirit of the treatment of Lee, Rice and Anderson (hereafter referred to as LRA, [17]).

The starting point for any non-correlated theory of electron–phonon interaction is the Fröhlich Hamiltonian

$$H = \sum_k \epsilon(k) c_k^\dagger c_k + \sum_q \omega(q) b_q^\dagger b_q + \frac{1}{\sqrt{L}} \sum_{q,k} g(q) c_{k+q}^\dagger c_k u_q$$

$$u_q = \frac{1}{\sqrt{2\omega(q)}} (b_q^\dagger + b_{-q})$$
(1)

where c_k^\dagger and b_q^\dagger are (respectively) creation operators for electrons and phonons with dispersion $\epsilon(k)$ and $\omega(q)$, u_q is the Fourier transform of the lattice displacement, and $g(q)$ the electron–ion coupling. L is the number of sites. For simplicity we will not credit the electrons with spin, and will describe the band by a free-particle dispersion relation, linearized about k_f .

Consideration of the linear response of this system [14] reveals that the phonon frequencies undergo drastic adjustment if the band is near half-filling; the $2k_f$ -phonon is softened and its frequency vanishes at a well defined mean-field transition temperature T_c given by

$$k_B T_c = \frac{2\gamma}{\pi} e^{-1/\lambda} v_f k_f$$
(2)

with

$$\lambda = N_0 \frac{|g(2k_F)|^2}{\hbar^2 \omega_{2k_F}^2}$$
(3)

where N_0 is the density of states at the Fermi energy, and $\gamma \approx 0.5772$ is Euler’s constant. The overall picture of the important quantities in the mean-field theory is presented in

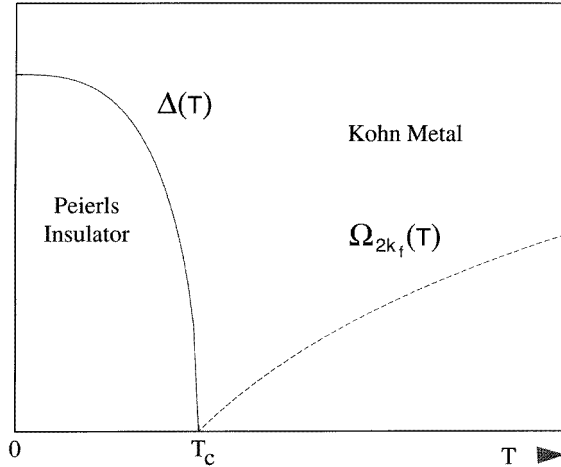


Figure 1. Phases of a Peierls insulator—from a Kohn metal with phonon frequency Ω_{2k_f} to a band insulator with gap $\Delta(T)$.

figure 1, where the gap $\Delta(T)$ and the phonon frequency $\omega_{2k_f}(T)$ are plotted on a phase diagram.

The result in equation (2) (the giant Kohn effect) may also be found in low-order perturbation theory, in which case a length scale ξ_0 emerges naturally from the calculation:

$$\xi_0 = \frac{\sqrt{7\zeta(3)}v_F}{4\pi k_B T_c} \quad (4)$$

where $\zeta(3) \approx 1.202$ is the Riemann zeta function, and v_F the Fermi velocity. Condensation of the softened $2k_F$ -phonon leads to a static lattice distortion $\langle u_{2k_F} \rangle$, and the opening of a gap Δ in the electronic spectrum. The interaction term in the Fröhlich Hamiltonian (1) may then be approximated by a BCS-like mean-field form

$$H_{ep}^{(MF)} = \sum_k [\Delta^* c_{k-2k_F}^\dagger c_k + \Delta c_{-k+2k_F}^\dagger c_{-k}] \quad (5)$$

$$\Delta = \frac{1}{\sqrt{L}} g(2k_F) \langle u_{2k_F} \rangle.$$

Self-consistent solutions for Δ and $\langle u_{2k_F} \rangle$ as a function of temperature may now be found for the Peierls insulator in the same way as for a BCS superconductor. Both systems are dominated by the same square-root singularity in the electronic density of states at the edges of the gap.

This picture of a metal–insulator transition in a purely one-dimensional metal is clearly not adequate as we expect fluctuations of the order parameter, when properly accounted for, to destroy the mean-field solution at *any* finite temperature. Real systems, however, are not truly one-dimensional. $(\text{TaSe}_4)_2\text{I}$ comprises parallel chains of tantalum atoms [20], surrounded by approximately perpendicular rectangles of Se (figure 2). The iodine resides between chains. Overlapping d_z orbitals on the tantalum chains form a band along which conduction occurs. Whilst electronic transport across the chains is believed to be diffusive at the temperatures of interest here and thus does not give rise to coherent dispersion in the perpendicular directions, interchain interactions can act to stabilize the mean-field solution at some three-dimensional ordering temperature T_c^{3D} considerably less than the mean-field

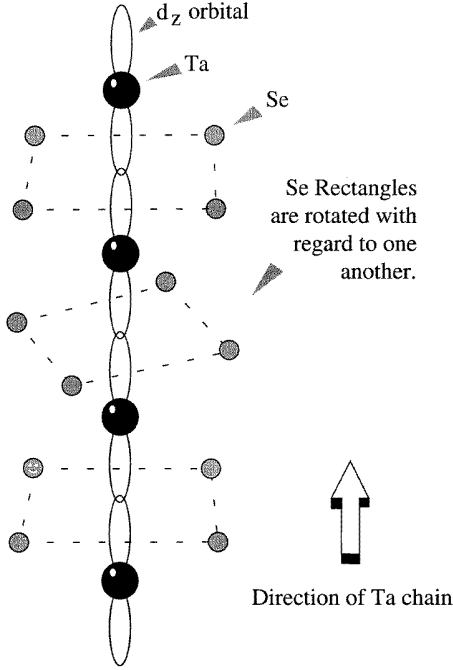


Figure 2. The schematic structure of the Ta chain in $(TaSe_4)_2I$.

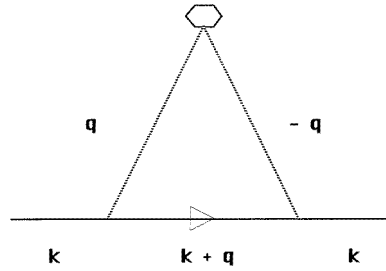


Figure 3. A Feynman diagram for the electron self-energy in the LRA theory, with the phonon self-energy indicated by the lozenge.

temperature T_c . This then corresponds to the transition observed in real systems. The LRA model of a one-dimensional metal does not explicitly include interchain effects, but their relevance and the three-dimensional ordering temperature emerge very naturally from their analysis. It is found that $T_c^{3D} \approx T_c/4$.

The physical content of Lee, Rice and Anderson's extension of the mean-field picture is the realization that the $2k_f$ -fluctuations of the softened lattice are slow on the time-scale of electron dynamics and that they may therefore be approximated by a static disorder potential, the determination of which is then a separate (classical) problem.

We start, then, from a natural generalization of the BCS approximation to the electron-phonon interaction

$$\bar{H}_{ep} = \sum_{Q, k' > 0} [\Psi_{-Q}^* c_{k'-Q}^\dagger c_{k'} + \Psi_Q c_{-k'+Q}^\dagger c_{-k'}] \quad (6)$$

where

$$\Psi_Q = \frac{1}{\sqrt{L}} g(Q) u_Q \quad (7)$$

are the components of the disorder potential and may be likened to an order parameter for fluctuations of some portion of the lattice. LRA then prescribe an equation-of-motion treatment of this Hamiltonian, which after certain approximations generates the following relation for the electronic Green's function:

$$\mathcal{G}(k, k; i\omega_n)^{-1} = \epsilon(k) - i\omega_n - \sum_Q \Psi_Q \Psi_{-Q}^* \frac{1}{\epsilon(k-Q) - i\omega_n}. \quad (8)$$

The same relation may be written down immediately by using the analogy with static disorder simply to calculate the second-order self-energy correction for electrons scattered by the potential Ψ_Q [18]. The Feynman diagram used is shown in figure 3. The lozenge in the diagram is the phonon self-energy, or the charge–charge correlation function at $2k_F$. The deformed lattice approximation treats the ionic configuration as rigid (incapable of recoil), with the positions given by a thermal average. The absence of a frequency sum in the electron self-energy expresses the fact that the lattice and CDW fluctuations have been decoupled.

We note in passing that it would in principle be possible to substitute a Luttinger-liquid Green's function in the expression for the self-energy, and so to treat the effects of lattice distortion on a correlated system to a similar level of approximation. To obtain and parametrize spectral functions from such a calculation would not, however, be trivial. Similarly, refinements may be made to allow for lattice recoil. We shall not present these here, but will limit our discussion to the Green's function previously found by LRA.

Evaluation of this expression then requires knowledge of the correlation function for the lattice fluctuations at a given temperature. A means of finding this was supplied by Scalapino, Sears and Ferrell [19]. They perform a functional minimization of a generalized Ginzburg–Landau free energy to obtain correlation functions for a fluctuating order parameter in a one-dimensional system, and obtain the following form:

$$\langle \Psi(x)\Psi(x') \rangle = \langle \Psi^2(T) \rangle \exp[-|x - x'| \xi^{-1}(T)] \cos[2k_F(x - x')]. \quad (9)$$

LRA substitute a free energy with parameters taken from the mean-field (linear response) perturbative treatment of the 1D Fröhlich Hamiltonian:

$$F[\Psi_Q] = a(T)|\Psi_Q|^2 + b(T)|\Psi_Q|^4 + c(T)(Q - 2k_F)^2|\Psi_Q|^2 \quad (10)$$

with

$$a(T) = D_0 \frac{T - T_c}{T} b(T) = D_0 \left[b_0 + (b_0 - b_1) \frac{T}{T_c} \right]$$

and

$$c(T) = D_0 \xi_0^2(T)$$

where D_0 is the (constant) density of states for the band, which is taken to have width $2\epsilon_F$. We fix b_0 and b_1 to give the correct zero-temperature value of the gap Δ_0 in the electronic spectrum: $b_0 = 1/2\Delta_0^2$ and

$$b_1 = b_0 \frac{7\zeta(3)}{16\pi} \frac{(1.76)^2}{0.5}.$$

The problem of determining $\langle \Psi_Q^2(T) \rangle$ and $\xi(T)$ then reduces to that of finding the low-lying energy levels of a particle moving in an anharmonic potential well, the shape of which is determined by the coefficients of the free energy:

$$H = -\frac{1}{4} \frac{k_B^2 T_c^2}{D_0} \frac{\partial^2 \Psi}{\partial x^2} + a(T)|\Psi|^2 + b(T)|\Psi|^4. \quad (11)$$

This may be solved numerically, or approximately using perturbation theory and asymptotic analysis. It is found that the coherence length ξ increases steadily from its mean-field value at T_c with reducing temperature, but increases very rapidly at a temperature approximately one quarter of T_c . This implies that long-range order exists for temperatures below $\frac{1}{4}T_c$, and interchain coupling stabilizes the mean-field solution. We will identify this temperature with the transition temperature T_c^{3D} of a three-dimensional system and not attempt to

treat interchain effects explicitly. The mean square value of the correlations increases approximately linearly with decreasing temperature, and takes on the role of a mean-field gap below the three-dimensional ordering temperature.

The following parametrization is accurate in the temperature range of experimental interest in the next section:

$$\xi^{-1}(T) = \xi_0^{-1}(T) \left(\frac{4T}{3T_c} - \frac{1}{3} \right) \quad (12)$$

$$\langle \Psi^2(T) \rangle = \frac{a'}{b} \left(1 - \frac{T}{T_c} \right) - \frac{1}{2} k_B = \frac{T_c}{a'} \frac{1}{\sqrt{1 - T/T_c}} \quad (13)$$

where $a' = a(T)/T$.

We are now in a position to assemble the Green's function for the system, with the (static) lattice fluctuations parametrized by the 'gap' (squared) energy scale $\langle \Psi^2(T) \rangle$ and the 'lifetime' energy scale $\xi^{-1}(T)$:

$$G_R(k, k; \omega)^{-1} = \omega - \epsilon(k) - \int dQ \frac{S(Q) \langle \Psi^2 \rangle}{\omega - \epsilon(k_{\pm}^+ Q) + i\delta} \quad (14)$$

where $S(Q)$ is a Lorentzian of width ξ^{-1} centred on $Q = 2k_F$, the sign in the denominator is chosen to give $\epsilon(k_{\pm}^+ Q) \sim \epsilon(k)$, and $\langle \Psi^2 \rangle$ is found from the results of SSF [19]. Evaluating the integral over Q , and dropping the second momentum index, we arrive at a result for the Green's function:

$$G_R(k, \omega) = \frac{\omega + \epsilon(k) + i v_F \xi^{-1}}{\omega^2 - \epsilon(k)^2 - \langle \Psi^2 \rangle + i v_F \xi^{-1} (\omega - \epsilon(k))}. \quad (15)$$

This will form the basis for most of the subsequent analysis.

3. Basic properties of the model

Insight into the properties of the model outlined may be obtained by consideration of the imaginary part of the Green's function (15) derived above:

$$A(k, \omega) = \frac{v_F \xi^{-1} \langle \Psi^2 \rangle}{[\omega^2 - \epsilon(k)^2 - \langle \Psi^2 \rangle]^2 + v_F^2 \xi^{-2} [\omega - \epsilon(k)]^2} \quad (16)$$

where the parameters $\langle \Psi^2 \rangle$ and ξ^{-1} have the scale and temperature dependence given above. As observed by LRA, this may be integrated analytically to give an expression for the density of states. This is plotted for a system at temperature $T = 300$ K with $T_c = 892$ K, $T_c^{3D} = 263$ K and $\epsilon_F = 1.2$ eV in figure 4; the reason for this choice of parameters will be discussed in the light of photoemission data in a later section.

The density of states shows clear evidence of a quasigap at all temperatures above T_c^{3D} observable for a system such as $(\text{TaSe}_4)_2\text{I}$. Spectral weight *is* still present at the Fermi energy ($\omega = 0$) at room temperature, but is greatly reduced. Traces of the square-root singularity which will dominate the mean-field solution are visible at the edges of the gap for temperatures approaching T_c^{3D} . Sharp spikes and edges in the plot are a numerical artifact only.

The LRA Green's function (15) above can clearly be seen to reduce to a BCS-type Green's function:

$$G_R(k, \omega) = \frac{\omega + \epsilon(k)}{\omega^2 - \epsilon(k)^2 - \langle \Psi^2 \rangle + i\delta} \quad (17)$$

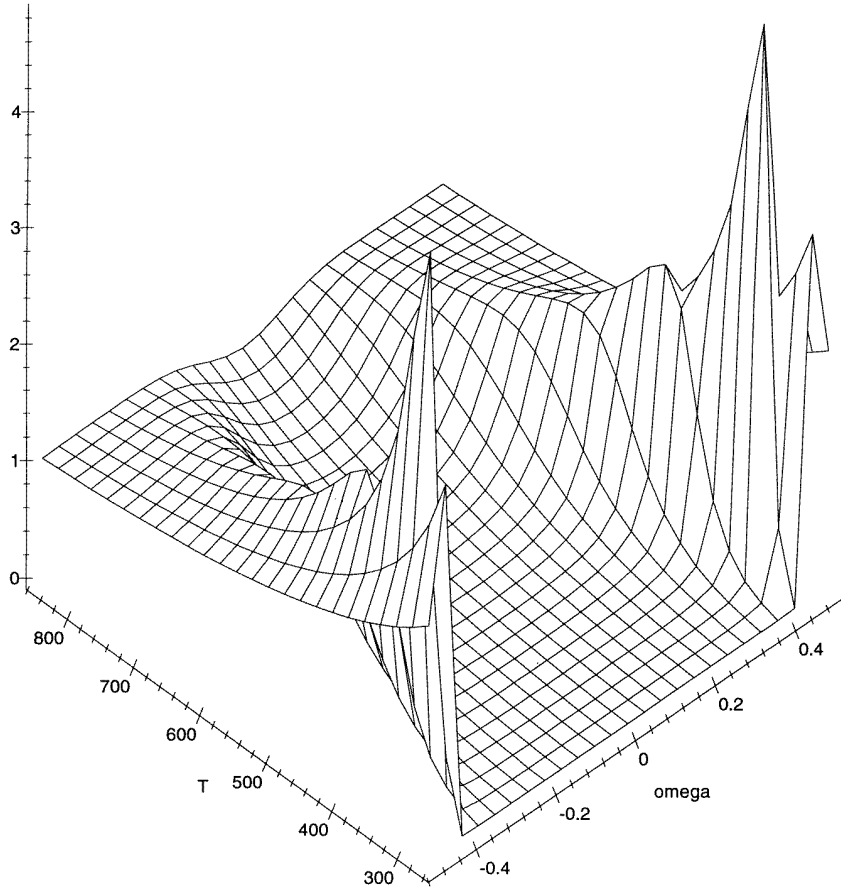


Figure 4. The LRA density of states as a function of energy and temperature for the conducting phase.

with $\langle \Psi^2 \rangle$ taking on the role of a real gap in the limit where $\xi \rightarrow \infty$; this mean-field solution is in fact the exact zero-temperature limit of the LRA theory. At the level of approximation relevant to the experiments the model may be taken to possess a real gap below T_c^{3D} . We shall then proceed to describe the system by an LRA Green's function (15) above T_c^{3D} (263 K for $(\text{TaSe}_4)_2\text{I}$), and by a BCS Green's function below T_c^{3D} .

It is also possible to integrate the spectral function numerically over ω to obtain a result for $n(k)$. (The integration may be performed analytically for the BCS-like expression below T_c^{3D} .) This is displayed in figure 5. The occupation number is clearly dominated by the presence of the quasigap, varying over a scale in k -space given by $\Delta/\hbar v_F$. No Fermi step is present in the occupation number at an experimentally observable temperature, but the region of k -space over which $n(k)$ undergoes most change becomes *smaller* with increasing temperature and decreasing size of the quasigap. Both the occupation number and the density of states illustrate the fact that the metallic (fluctuating CDW) phase of the model does not resemble a conventional Fermi liquid.

Consideration of the denominator of the spectral function at k_F shows that spectral weight is concentrated in one peak provided that the quantity $\langle \Psi^2 \rangle - v_F^2 \xi^{-2}/4$ is negative.

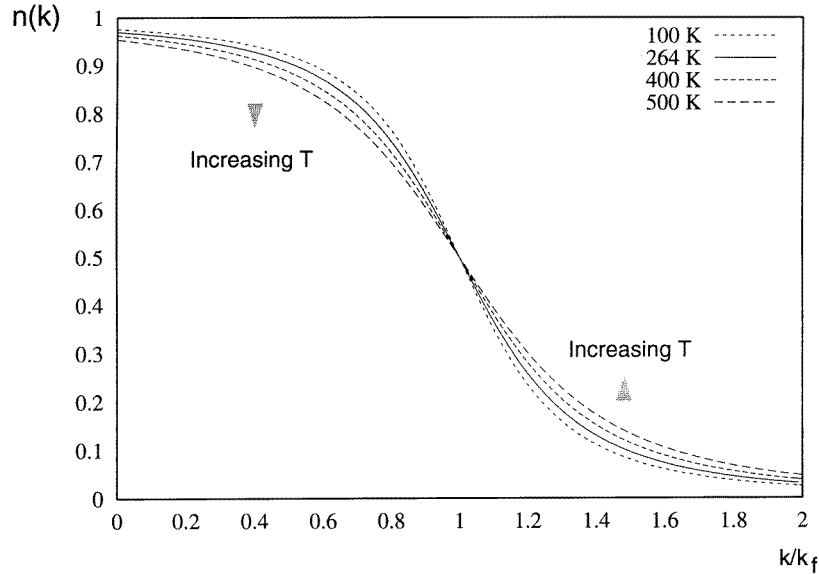


Figure 5. A plot of $n(k)$, the occupation number, for temperatures above, below, and at (solid line) the 3D ordering temperature.

This gap-like parameter will change sign at a temperature of similar magnitude to, but in general different from, the mean-field temperature T_c . On cooling it becomes positive, and spectral weight is split into two peaks. Since T_c is well above room temperature, the two-peak structure is the only one expected in the experiments of the following section. The breadth of the peaks is determined by the inverse coherence length ξ^{-1} . At k_F the division of spectral weight between peaks is even; for k -vectors deeper in the valence band more weight is found in the lower peak. This may be compared directly with coherence factor effects in the BCS-like phase of the model below T_c^{3D} . The opening of the quasigap in the density of states is visible then in $A(k, \omega)$ as a splitting of spectral weight into two broad peaks, and the transition from metal to insulator marked by the progressive narrowing of these peaks until they become delta functions separated by a real gap at T_c^{3D} . Tight bunching of peaks near the edges of the gap lead to the pronounced rise in the density of states there; this will again resolve into a square-root divergence below T_c^{3D} .

4. Angle-resolved photoemission

Quasi-one-dimensional materials were chosen for angle-resolved photoemission experiments on account of the interesting phase transitions which they undergo, and also because the reduced dimensional nature of their Brillouin zones simplified the interpretation of the spectra obtained. The existence of many exactly soluble models of one-dimensional systems makes the exploration of quasi-one-dimensional materials equally appealing from a theoretical point of view. The particular hope of finding evidence for the existence of a Luttinger liquid has motivated a large number of photoemission studies of quasi-one-dimensional conductors. Among these, the most detailed studies have been performed on $(\text{TaSe}_4)_2\text{I}$, [10, 11, 22], and the discussion of the data on this compound is our object in

this section.

While the authors of the papers on $(\text{TaSe}_2)_4\text{I}$ often disagree on the detailed interpretation of their data, the lack of spectral weight at the Fermi energy is a universally observed trend. As this is one of the signal features of a Luttinger liquid, several researchers have concluded that $(\text{TaSe}_4)_2\text{I}$ and its sister compounds are Luttinger liquids in their conducting phase. The nature of the loss of spectral weight may be best probed by angle-resolved photoemission, since this offers some hope of establishing whether the missing weight has moved.

The quantity measured by an ideal angle-resolved photoemission experiment at zero temperature is the ground-state electronic spectral function of the material being probed. This is formally equivalent to the imaginary part of the system's retarded Green's function, and so confers complete knowledge of its single-particle properties. Real photoemission experiments suffer limitations of finite temperature and resolution, and can only probe the properties of the surface layer of material from which the electron emerges. Spectra also contain a substantial systematic background, which is not generally well understood, and which must be subtracted according to some prescription before the data can be fully analysed.

Recent angle-resolved studies of the conduction band in $(\text{TaSe}_2)_4\text{I}$ have been performed above and below its CDW transition temperature, and the spectra possess a number of interesting features. The one most stressed in the literature is the lack of spectral weight at and near the Fermi energy. Related to this is the lack of a Fermi step in the background of spectra taken *above* the transition temperature. These features represent a marked departure from the usual character of metallic conduction, as observed in similar experiments on three-dimensional systems. We shall see below that there are several other characteristics of the experimental results that are similarly anomalous.

The simplest result (non-interacting electrons) for energy-distribution curves (EDCs) in ARPES done for initial electron momentum near the Fermi energy would be a delta function. Finite experimental resolution will of course broaden this peak. We have convoluted our results with a Gaussian resolution function. The width is equal to the published estimated resolution of 160 meV. One source of (not very interesting) background is that of secondary electrons. The intensity of this rises steeply as the detected energy decreases, starting a few eV below the Fermi energy. It was found that, for each spectrum, a Gaussian with width of similar order to that of the band and centred at an energy below the band minimum could be chosen to closely mimic this contribution, and this was duly subtracted. The overlap of the Gaussian with the interesting structures near the Fermi energy is small, but due to its width not quite negligible.

As a rule, however, the most striking difference between observed EDCs and the ideal result is the existence of a structure resembling a Fermi edge in addition to the expected peak. This should be attributed to the existence of quasi-elastic scattering of electrons on exit from the sample, probably arising from disorder near the surface. It is important to remember that electrons detected in ARPES originate from near the surface and few surfaces are atomically flat. To take this into account, it is most reasonable to suppose that some fraction of the electrons have their momenta randomized on exit.

The resulting spectrum is a linear combination of a true angle-resolved spectrum (the spectral function), and an angle-integrated spectrum (the density of states). In theoretical terms, this means a combination of the imaginary part of the one-particle Green's function and the imaginary part of its trace. This picture is confirmed by the observation that ARPES EDCs and angle-integrated spectra taken on a single sample do differ only by the peak structure in the former. The relative weight in the two components must be determined by a fit.

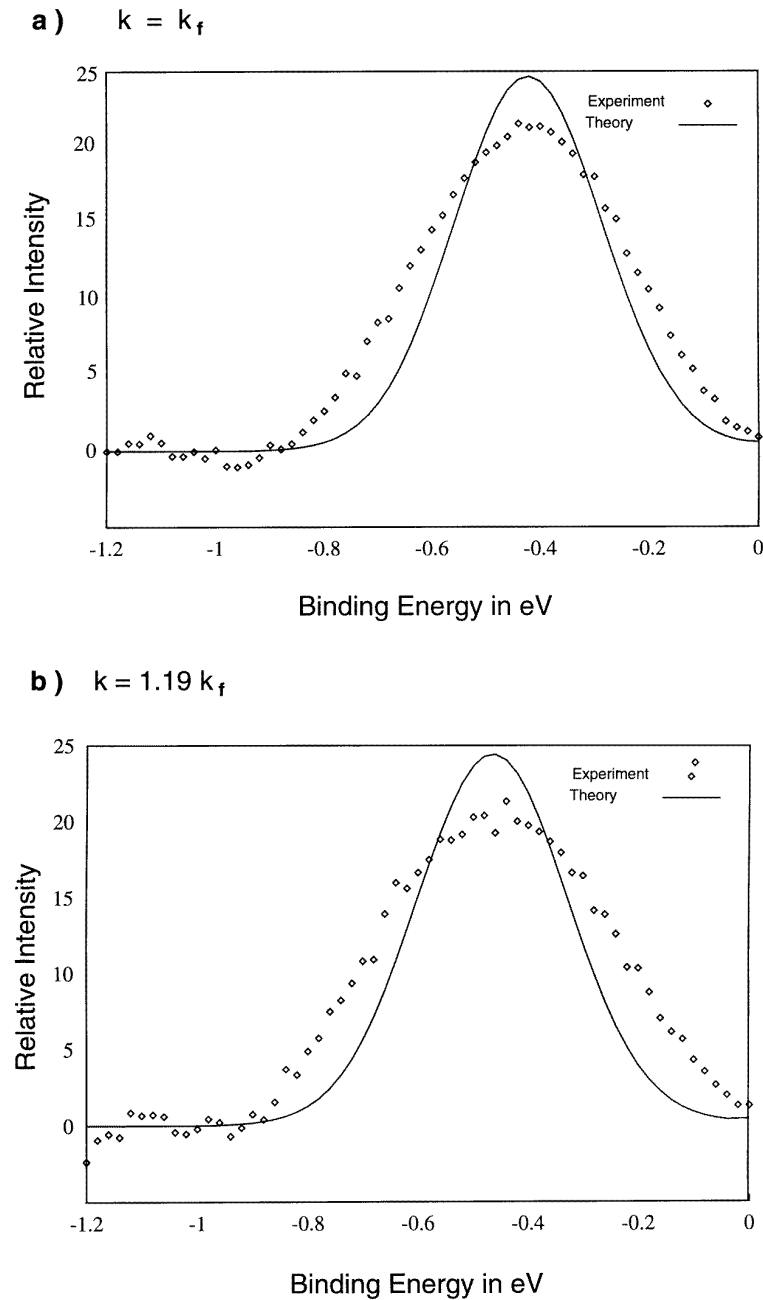


Figure 6. Single-parameter fits to ARPES spectra taken on $(\text{TaSe}_4)_2\text{I}$ in the conducting phase, for various wavevectors for which data were available.

The experiments on $(\text{TaSe}_4)_2\text{I}$ fit this picture, with one exception. In contrast to experiments on three-dimensional metals, the angle-integrated spectrum near the Fermi energy does not resemble the expected Fermi function. Instead, the occupation falls off smoothly in the neighbourhood of the chemical potential. Qualitatively, this may be the

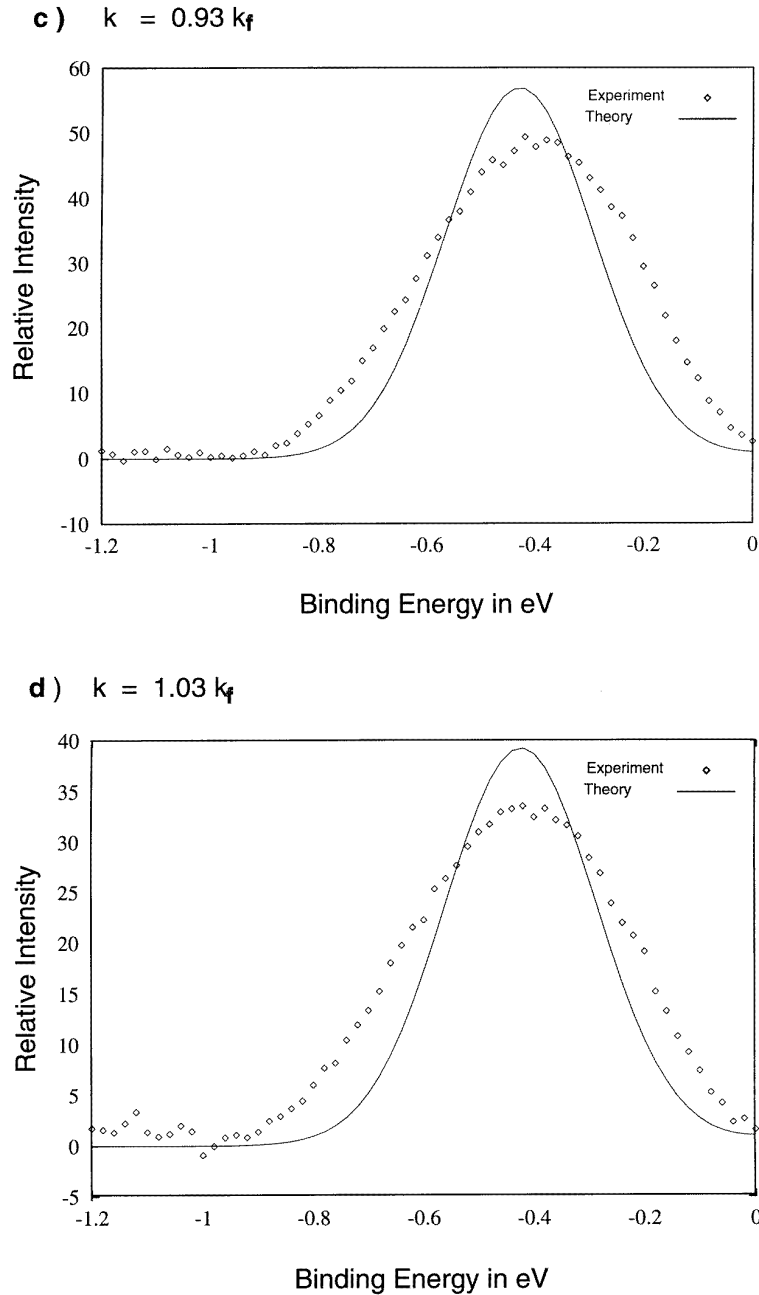
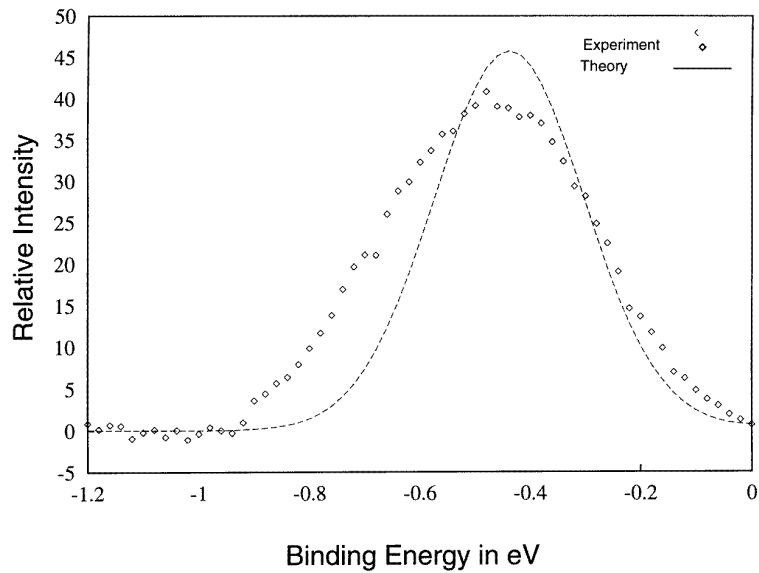


Figure 6. (Continued)

result of Luttinger-liquid behaviour. However, it may also result from the pseudogap in the LRA theory. Only a quantitative comparison can distinguish these alternatives.

We show the comparison of experiment and theory in figure 6. Each plot is taken at a fixed angle of outgoing electron, and the inferred wavevectors are as shown. The

e) $k = -0.89 k_f$



f) : $k = -1.15 k_f$

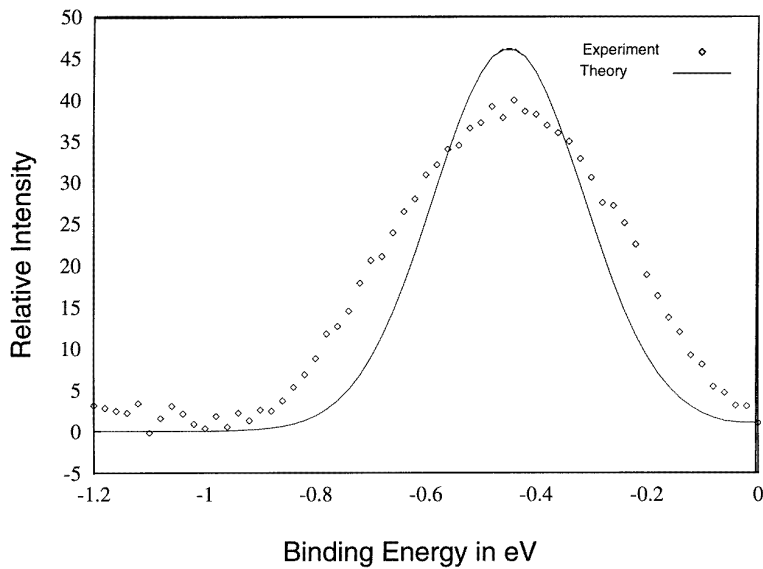


Figure 6. (Continued)

data are taken from reference [21]. The choice of wavevectors shown was dictated by the availability of experimental data. The background, fitted by a Gaussian as mentioned above, has already been subtracted from the experimental curves. The theoretical curves are plotted from equation (16), broadened by convolution with the Gaussian resolution function. Two

free parameters were retained for the fit: the mean-field transition temperature with a best-fit value $T_c = 892$ K and the Fermi velocity $v_F = 6.5 \times 10^5$ m s⁻¹, which is fixed by the overall linear dispersion. The parameter $k_F = 0.27 \text{ \AA}^{-1}$ is fixed by the fact that the band is one quarter filled. This gives a zero-temperature gap $\Delta_0 = 0.52$ eV by extrapolation of the dispersion to low temperatures. T_c compares well with the expectation that, at a temperature around $T_c/4$, the actual transition should take place and the resistivity should become activated. In (TaSe₄)₂I this occurs at $T_c^{3D} = 263$ K.

Each plot shows a peak broader than the experimental resolution of 160 meV. The fits have been made with the stated resolution. It is evident that extremely good fits could be made either by increasing the width of the convolving function by about 50 meV (30%), by assuming some scattering of the electrons as they exit the material, or by assuming that the material is impure to begin with, which would give a momentum-independent additional width to the spectral function. Since all three of these alternatives involve the introduction of an *ad hoc* parameter, we have preferred to leave the theoretical curves as shown and merely note that it would be somewhat surprising if there was no source of broadening beyond the instrumental resolution and that in equation (16).

Evaluating the comparisons in figure 6, we may say that the peak positions are given very well. The worst case is figure 6(c), where the theoretical prediction is too low by perhaps 30 meV, and the other discrepancies are smaller. The widths are too large by about 20% in all cases, suggesting some relatively minor additional systematic effect.

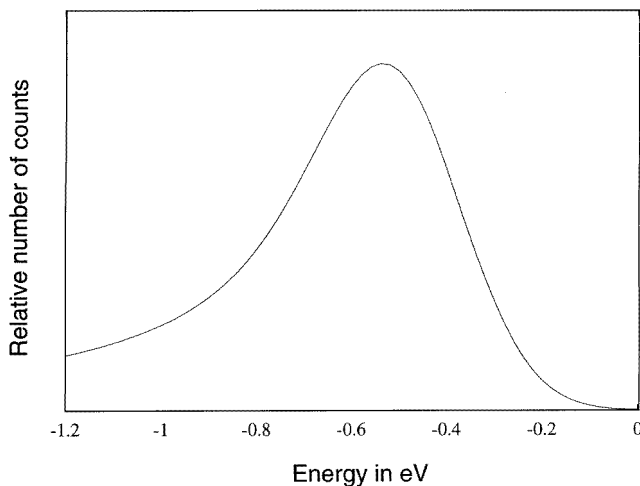


Figure 7. A momentum-integrated spectrum found from the LRA model in the conducting phase, showing suppression of the density of states at the chemical potential $\mu = 0$.

The momentum-integrated spectrum in figure 7 is obtained by integrating equation (16) over k . It may be compared with the results of angle-integrated experiments [10, 11], and is clearly in good qualitative agreement with these, although the limited validity of our linear approximation to the free-electron dispersion renders quantitative comparison away from the Fermi energy impossible. Most significant is the movement of weight away from the Fermi energy, the signature of the pseudogap caused by the charge fluctuations.

5. Fermi liquid, Luttinger liquid, or LRA liquid?

Four features of the LRA theory *and* the data are striking.

(1) The movement of the peak position as a function of momentum is very small near k_F . In fact, the dispersion relation, if it is defined as the peak position, apparently nears a quadratic maximum at k_F .

(2) The peaks are broad and symmetric. The widths are not very momentum dependent, ranging only from about 400–600 meV in the range under study.

(3) There is a strong pseudogap at all momenta, with the weight of the spectral function at the Fermi energy small. In addition, there is clear evidence of an energy scale associated with the gap structure. This is best read off from the peak position in figure 7 as about 500 meV. This is related to the zero-temperature CDW gap in the LRA theory.

(4) There are what may be called ‘shadow bands’. These are electronic states, or rather peaks in the spectral function, where no bands should be in a free-electron picture. In the data, a clear peak is seen even at momenta $|k| > k_F$. These peaks shadow the ordinary band in the range $|k| < k_F$ —they are translates of the ordinary peaks through $\pm 2k_F$.

On all four points the data agree qualitatively, and even semiquantitatively, with the LRA theory.

Let us first compare these findings with the expectations of Fermi-liquid theory. The spectral function should approach

$$A(k, \omega) \sim \delta(\omega - v_F(k - k_F)) \quad (18)$$

as k approaches k_F . Further from k_F , we expect broadening due to interactions proportional to ω^2 . Specifically:

- (1)' in a Fermi liquid, the peak should disperse linearly through the Fermi momentum;
- (2)' the peak should be symmetric, and the width should be resolution limited at k_F and broaden away from k_F ;
- (3)' there is no gap or pseudogap and the only energy scales are $\epsilon_F > 1$ eV and $k_B T \approx 30$ meV;
- (4)' there are no peaks when $k > k_F$.

It is clear, comparing points (1)' to (4)' to experiment (1) to (4), that this simple Fermi-liquid behaviour is not at all consistent with the observations.

In the Luttinger liquid, we have a very different form for the spectral function at low energies. In the spinless case [23], the delta function characteristic of the Fermi liquid is replaced by a power-law singularity:

$$A(k, \omega) \sim \Theta(\omega + \tilde{v}_F|(k - k_F)|)(-\omega + \tilde{v}_F(k - k_F))^{\gamma-1}(-\omega - \tilde{v}_F(k - k_F))^\gamma. \quad (19)$$

In this formula, Θ denotes the step function: $\Theta(x) = 0$ for $x < 0$, and $\Theta(x) = 1$ for $x > 0$. $\hbar\omega$ is the energy measured relative to the chemical potential so that $\omega < 0$ for initial electron energies less than the chemical potential. γ is the coupling strength for the electron–electron interaction. For short- (finite-) range interactions we expect $0 < \gamma < 1$, (the infinite- U Hubbard model has $\gamma = \frac{1}{8}$ [24]). Here \tilde{v}_F is the excitation velocity, which includes contributions from the kinetic energy and the interaction. The integrated spectral function (density of states) has the low-energy form

$$\int A(k, \omega) dk \sim |\omega|^{2\gamma}. \quad (20)$$

In the case of electrons with spin, there are generally two singularities [25], one associated with the charge excitations at $\omega = \tilde{v}_{F,c}(k - k_F)$ and one associated with the spin excitations

at $\omega = \tilde{v}_{F,s}(k - k_F)$. If the velocities of the two sorts of excitation are very similar, then at finite resolution it may be difficult to distinguish this case from the spinless case. We may now compare the Luttinger-liquid scenario to experiment.

(1)'' In a Luttinger-liquid, for $\gamma < 1$ the singularity or singularities disperse linearly through the Fermi energy. For $\gamma > 1$, the dispersing structure becomes very diffuse near the Fermi energy.

(2)'' The widths that should be observed in a real experiment are not universal—they depend on the details of the interaction [26]. One would expect some asymmetry in the peaks, however.

(3)'' There is a pseudogap-like feature in the density of states. However, the exponent needed to fit experiment is larger than expected [26]. There is no obvious energy scale in the theory for repulsive interactions, though a peak may be observed in the density of states for [27] attractive interactions.

(4)'' There can be peaks for $\omega < 0$ and $k > k_F$. However, they would be expected to be rather insignificant if $0 < \gamma < 1$.

Here it appears that (1)'', and probably the asymmetry in (2)'' and the exponent in (3)'' are serious problems for the theory.

We conclude that the ARPES data on $(\text{TaSe}_4)_2\text{I}$ are not consistent with either a Fermi-liquid picture or a Luttinger-liquid picture.

The most decisive observation is the failure of the peaks in the EDCs to disperse through the Fermi energy. The shapes and the widths of the peaks as a function of momentum are also difficult to reconcile with these theories. The picture of very strong charge-density fluctuations at $2k_F$ appears, in contrast, to offer a consistent interpretation of all of the data. We note, however, that the value of the CDW gap extracted from photoemission is larger than that obtained from optical conductivity or resistivity measurements.

Efforts have been made in the last few years to obtain spectral predictions for the Luther–Emery model [28]. This provides a more natural framework for consideration of the materials in question, since CDW fluctuations are not expected to coexist with a Luttinger liquid. There is not yet, however, a universally agreed prediction which may be compared with experiment, and the lack of a simple energy scale in the model makes it difficult to extract quantitative information from the real spectra. It has also been brought to our attention since completion of this work, that a more complete and self-consistent treatment of electron–phonon interaction has recently been developed by McKenzie [29]. A striking feature of his theory is the asymmetry of the dispersing peaks in the spectral function, which is almost redolent of the Luttinger liquid, although quite different in its physical origin. We have not attempted to make a quantitative comparison of McKenzie's spectral function with the photoemission data for $(\text{TaSe}_4)_2\text{I}$, but note that there is no observable asymmetry in the data.

It must be stressed that these conclusions apply to this particular system only; experiments performed on other quasi-one-dimensional systems suggest that the relative importance of electron–electron and electron–phonon interaction effects is strongly dependent on the system in question. Even for $(\text{TaSe}_4)_2\text{I}$, correlation effects may be masked by the strong charge fluctuations only within a particular parameter regime; it is for example possible that the application of pressure to the chains would relatively strengthen the interaction effects. In other materials, and particularly in some of the quasi-one-dimensional SDW compounds, there would appear to be evidence for strongly one-dimensional correlation effects.

Acknowledgments

This work was supported by the National Science Foundation under Grant No DMR-9214739. We would like to thank A Chubukov, J Voit, V Meden, J Ma, F Mila, M Onellion and C Quitmann for useful discussions. We are particularly grateful to the authors of reference [21] for discussions of their data and for supplying it to us in digitized form.

References

- [1] Gressier P, Guemas L and Meerschaut A 1982 *Acta. Crystallogr. B* **38** 2877
- [2] Fujishita H, Sato M and Hosino S 1984 *Solid State Commun.* **49** 313
- [3] Fujishita H, Sato M, Shapiro S M and Hosino S 1986 *Physica B* **143** 201
- [4] Rocau C, Ayroles R, Gressier P and Meerschaut A 1984 *J. Phys. C: Solid State Phys.* **17** 2293
- [5] Sato E, Ohtake K, Yamamoto R, Doyama M, Mori T, Soda K, Suga S and Endo K 1985 *Solid State Commun.* **55** 1049
- [6] Geserich H P, Scheiber G, Dürrler M, Lévy F and Monceau P 1986 *Physica B* **143** 198
- [7] Berner D, Scheiber G, Gaymann A, Geserich H M, Monceau P and Levy F 1993 *J. Physique IV* **3** 255
- [8] Wang Z Z, Saint-Lager M C, Monceau P, Renard M, Gressier P, Meerschaut A, Guemas L and Rouxel J 1983 *Solid State Commun.* **46** 325
- [9] Johnston D C, Maki M and Grüner G 1985 *Solid State Commun.* **53** 5
- [10] Dardel B, Malterre D, Grioni M, Weibel P and Baer Y 1991 *Phys. Rev. Lett.* **67** 3144
- [11] Dardel B, Malterre D, Grioni M, Weibel P, Baer Y, Voit J and Jérôme D 1993 *Europhys. Lett.* **24** 687
- [12] Purdie D, Collins I R, Berger H, Margaritondo G and Reihl B 1994 *Phys. Rev. B* **50** 12222
- [13] Peierls R 1953 *Quantum Theory of Solids* (Oxford: Oxford University Press)
- [14] Rice M J and Strässler S 1973 *Solid State Commun.* **13** 125
- [15] Schulz H J 1991 *Int. J. Mod. Phys. B* **5** 57
- [16] Anderson P W and Ren Y 1990 *Proc. Los Alamos Symp. on High Temperature Superconductivity* ed K Bedell *et al* (New York: Addison-Wesley)
- [17] Lee P, Rice T M and Anderson P W 1973 *Phys. Rev. Lett.* **31** 463
- [18] Mahan G D 1990 *Many Particle Physics* (New York: Plenum) p 262
- [19] Scalapino D J, Sears M and Ferrell R A 1972 *Phys. Rev. B* **6** 3409
- [20] Gressier P, Whangbo M H, Meerschaut A and Rouxel J 1984 *Inorg. Chem.* **23** 1221
- [21] Terrasi A, Marsi M, Berger H, Margaritondo G, Kelly R J and Onellion M 1995 *Phys. Rev. B* **52** 5592
- [22] Hwu Y, Almeras P, Marsi M, Berger H, Levy F, Grioni M, Malterre D and Margaritondo G 1992 *Phys. Rev. B* **46** 13 624
- [23] Theuman A 1967 *J. Math. Phys.* **8** 2460; 1976 *Phys. Lett.* **59A** 99
Luther A and Peschel I 1974 *Phys. Rev B* **9** 2911
Haldane F D M 1981 *J. Phys. C: Solid State Phys.* **14** 2585
- [24] Ogata M and Shiba H 1990 *Phys. Rev. B* **41** 2326
Parola A and Sorreila S 1990 *Phys. Rev. Lett.* **64** 1831
Schultz H 1990 *Phys. Rev. Lett.* **64** 2831
- [25] Meden V and Schönhammer K 1992 *Phys. Rev. B* **46** 1573
Voit J 1993 *Phys. Rev B* **47** 6740; 1993 *J. Phys. C: Solid State Phys.* **5** 8305
- [26] Schönhammer K and Meden V 1993 *Phys. Rev. B* **47** 16205
- [27] Schönhammer K and Meden V 1993 *J. Electron Spectrosc. Relat. Phenom.* **62** 225
- [28] Voit J and Meden V 1996 private communications
- [29] McKenzie R H 1995 *Phys. Rev. B* **52** 16428